Journal of Applied Mechanics and Technical Physics, Vol. 44, No. 1, pp. 114–121, 2003

STRESS DISTRIBUTION IN A SLIP TRACE OF DEFORMED Ni_3Ge SINGLE CRYSTALS

Yu. A. Abzaev and V. A. Starenchenko

UDC 539.4.015

The shear-stress distribution produced by distortion of Ni_3Ge *single crystals under compression is studied. The evolution of the dislocation structure during deformation of* Ni_3Ge *single crystals of various orientations* ([$\bar{2}$34], [$\bar{1}$11], [$\bar{1}$39], *and* [001]) *at* $T = 77$, 293, 523, 673, *and* 873 K *is analyzed. It was found that, up to failure strains, the dislocation structure is characterized by a uniform dislocation distribution. Regardless of the strain-axis orientation, the linear relation* $\tau = f(\rho^{0.5})$ *is valid for all the test temperatures except for* $T = 77$ K. *The deviation from the linear relation at* $T = 77$ K *is due to the suppressed thermally activated slip of dislocations in nonuniform-strain fragments at the specimen edges. In these fragments, the shear stresses are substantially reduced, and hence, the stresses produced by the dislocation cluster retard the development of slip in this trace.*

Key words: *dislocation cluster, single crystal, shear strain, shear stress.*

In Ni_3Ge single crystals deformed under compression, strain-fragmentation regions are formed as a result of specimen distortion during shear [1, 2]. The effect of distortion of specimens under compression on the distribution of applied shear stresses has not yet been studied, and their role in the interdislocation interaction is not understood.

The goal of this work is to study the effect of distortion of a specimen under compression and stresses caused by fragmentation at the specimen edge on the shear-stress distribution along slip traces.

We studied the evolution of the dislocation structure (DS) during deformation of Ni_3Ge single crystals of various orientations ([$\bar{2}$34], [$\bar{1}$11], [$\bar{1}$39], and [001]) at test temperatures $T = 77$, 293, 523, 673, and 873 K. In [3–10], it was found that the DS is characterized by a uniform dislocation distribution up to failure strains. Figure 1 shows the shear stresses τ versus the dislocation density ρ for all the orientations and test temperatures considered. One can see that the linear relation

$$\tau = \tau_F + \alpha G b \rho^{0.5} \tag{1}$$

holds for all values of T except for $T = 77$ K. Here τ_F is the stress of dislocation self-retardation, α is the parameter of interdislocation interaction, b is the magnitude of the Burgers vector of dislocations, and G is the shear modulus. As the temperature increases, the slope of the straight lines $\tau = f(\rho^{0.5})$ decreases. The temperature also affects the stress τ_F. Formula (1) approximates experimental data, which shows that the contact interdislocation interaction plays a dominant role in hardening of Ni_3Ge single crystals [11–23]. The conventional strain $\varepsilon_{\text{conv}}$, the contributions of the reactions τ_1 and stoppers of arbitrary types τ_2 to deformation resistance, the long-range stresses σ_1 caused by adjacent dislocations, the noncompensated fields σ_2, the stresses of dislocation self-retardation τ_F, and the shear stresses τ_{sh} for various test temperatures are listed in Tables 1–3 for the orientations [$\bar{1}$11], [$\bar{1}$39], and [$\bar{2}$34], respectively. The method for calculating these quantities for Ni_3Ge single crystals in the [001] orientation is described in [3]. The data that allow one to determine the confidence intervals with a significance level of 99% for reactions μ_1 and those for stoppers of arbitrary types μ_2 are also given in Tables 1–3. The confidence interval of contributions of reactions and stoppers is determined by the formulas $\tau_1 \pm \mu_1$ and $\tau_2 \pm \mu_2$, respectively. The dominant role in producing shear stresses is played by contact retardation of dislocations. We consider the additive contribution of various mechanisms of dislocation retardation. The contribution of stoppers of arbitrary types is much higher

Tomsk State Academy of Architecture and Construction Engineering, Tomsk 634003. Translated from Prikladnaya Mekhanika i Tekhnicheskaya Fizika, Vol. 44, No. 1, pp. 137–147, January–February, 2003. Original article submitted October 1, 2001; revision submitted April 25, 2002.

 0021-8944/03/4401-0114 $25.00

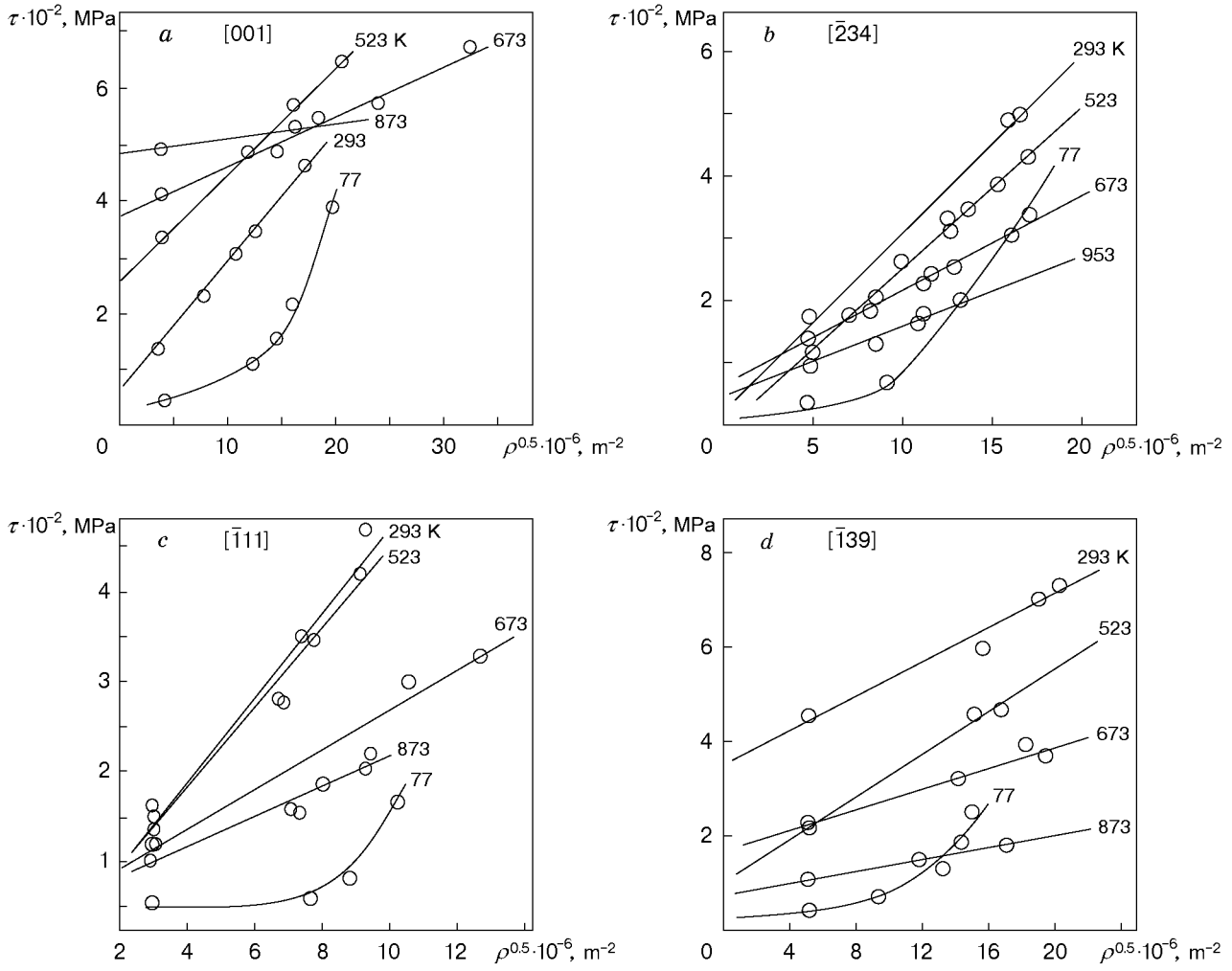

Fig. 1

than that of long-range stresses. The contribution of stoppers of arbitrary types is mainly due to reactions. The main part of shear stresses is composed of noncompensated long-range stresses and self-retardation of dislocations. The long-range fields produced by adjacent dislocations are negligible. It was found that the effect of deformation-resistance mechanisms varies with an increase in the test temperature. In the neighborhood of peak anomalous flow stresses, superposition of individual contributions is smaller than shear stresses. This can be explained by an increasing role of virtual rectilinear barriers [7, 8, 10]. However, the main contribution to deformation resistance is made by mechanisms of contact retardation of dislocations. An analysis of Tables 1–3 shows that shear stresses are determined by mechanisms whose action is proportional to the linear density of stoppers at the dislocation line. Elastic stress fields of dipoles, which can lead to deviation from relation (1), are insignificant part of shear stresses and decrease as strains increase [3]. The relation $\tau = f(\rho^{0.5})$ is nonlinear for all the orientations studied at $T = 77$ K (Fig. 1). An analysis of the slip-band pattern on the surface shows that rough slip occurs at $T = 77$ K. Similar results were obtained in [24]. At $T = 77$ K, thermally activated motion of dislocations is suppressed. Dislocations are appreciably attached to their slip plane. Slip fragmentation caused by distortion of single crystals with increasing strain shows that the external-stress distribution along the slip traces at the specimen edges is nonuniform [1, 2].

We consider the shear-stress distribution along the slip trace $LPDF$ (Fig. 2). Upon leaving the region of uniform strain at the point D, the dislocations in the slip plane continue to move as shear stresses decrease. They cease to move upon attaining a point in the trace at which the external stress approaches the yield point (point T in Fig. 2b). In the local volume considered, the shear stresses act on the upper surface only (Fig. 2a). On the lower surface, the stresses vanish along the strain axis. As a result, the trace of the slip system passes from the line DE

TABLE 1

T, K	$\varepsilon_{\text{conv}}$, %	τ_1, MPa	τ_2, MPa	σ_1, MPa	σ_2, MPa	μ_1, MPa	μ_2, MPa	τ_{sh}, MPa	τ_F, MPa
77	5.57	22.3	74.3	12.2	39.6	10.3	20.7	58.9	20
	10.13	12.9	69.0	10.2	43.0	7.8	21.2	80.4	
	19.5	28.2	75.6	14.4	36.2	9.2	14.9	165.8	
293	5	49.7	190	37.4	79.3	24.0	32.7	168.1	48.5
	10	84.6	198	56.8	98.1	36.3	40.0	312.0	
	16	55.6	229	51.5	121.0	30.2	46.9	328.0	
523	5	60.1	148	23.0	74.6	14.7	30.6	239.1	3.8
	10	48.0	119	22.2	77.7	13.4	31.2	295.1	
	16	103.0	223	62.5	113.0	40.0	44.4	352.2	
	21	110.0	286	69.4	142.0	40.8	53.7	150.6	
673	10	82.6	175	39.7	81.5	24.7	32.7	264.1	20
	15	94.1	226	39.2	132.0	25.1	53.6	340.8	
	21	119.0	253	48.6	132.0	31.1	41.0	472.0	
873	5	24.6	101	11.4	43.7	7.1	17.7	156.5	47
	11	39.5	112	24.2	57.9	15.0	23.8	153.3	
	18	48.3	110	18.4	66.1	11.4	27.6	221.0	
	30	53.3	138	32.4	82.7	27.6	34.5	212.3	

TABLE 2

T, K	$\varepsilon_{\text{conv}}$, %	τ_1, MPa	τ_2, MPa	σ_1, MPa	σ_2, MPa	μ_1, MPa	μ_2, MPa	τ_{sh}, MPa	τ_F, MPa
77	5	30	72	13	27	8	11	71.0	20
	10	38	92	16	28	4	11	154.4	
	18	76	148	35	68	21	20	250.0	
293	2.8	120	280	44	95	28	41	564.2	100
	5	150	260	43	73	26	29	696.2	
	7.8	170	300	46	88	27	35	911.6	
	11	190	370	54	110	32	36	1064.2	
523	2.45	73	150	49	55	15	22	585.9	348
	6.8	82	190	32	59	19	24	703.1	
	9	91	200	43	75	25	30	732.3	
673	2.3	42	100	21	41	13	16	322.9	167
	6.4	68	210	36	89	21	36	398.6	
	8.45	84	200	31	80	19	32	448.6	
873	4.8	39	83	24	38	13	15	186.2	74
	7.24	38	88	21	36	12	14	177.8	
	12.6	45	120	21	61	12	23	183.4	

TABLE 3

T, K	$\varepsilon_{\text{conv}}$, %	τ_1, MPa	τ_2, MPa	σ_1, MPa	σ_2, MPa	μ_1, MPa	μ_2, MPa	τ_{sh}, MPa	τ_F, MPa
77	5	24	56	13	26	8	10	90	10
	8	32	75	15	35	9	14	130	
	15.5	45	100	17	55	10	22	160	
77	24.65	40	130	21	69	13	27	260	32.4
293	6.5	63	130	29	72	18	30	271.2	32.4
	13.5	89	190	45	82	27	33	497	
293	16.5	130	250	67	120	39	49	503	1.7
523	5	44	110	32	49	11	21	162	1.7
	10.62	63	140	44	68	18	29	265	
	16.4	71	150	33	55	21	23	328	
	21.4	93	180	39	68	24	28	359	
	25.09	100	210	39	94	24	38	440	
673	5	41	77	21	34	13	15	181	67
	11.1	56	110	29	46	19	19	252	
	16.7	55	140	26	70	16	29	238	
	21.3	60	170	42	86	17	35	301.2	
873	6	22	69	13	38	8	16	127	54
	4.6	29	56	17	31	10	13	112.4	
	15.1	34	84	18	39	11	11	185	
	19	38	83	17	37	10	15	160	
	26.7	27	48	19	25	12	10	182	
	33.2	40	86	17	54	11	22	130.1	

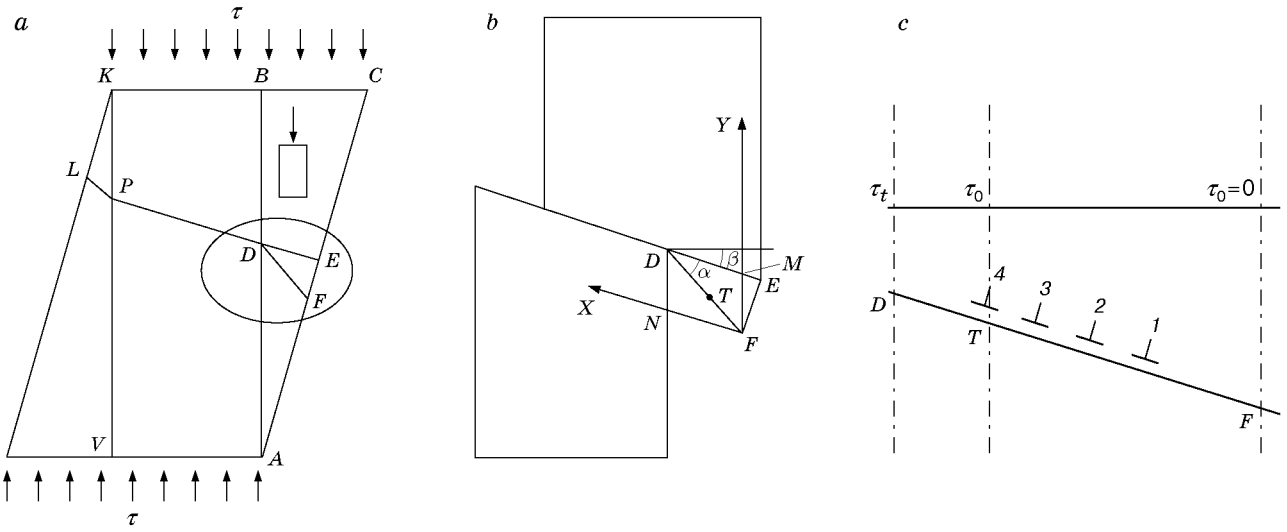

Fig. 2

to the line DF (Fig. 2a). Figure 2b shows the considered region DEF. Obviously, the slope of the line DE is determined by accumulated shear power DF. By virtue of uniformity, the shear stresses at different points of the trace PD in the region $ABKV$ (Fig. 2a) are identical and coincide with applied external stresses.

We now consider the shear-stress distribution along the trace DF. The final configuration of the region DEF (Fig. 2a) can be assumed to result from the following displacements. Under the action of stresses, the point N (Fig. 2b) is shifted to the point D. At the point F, the applied stresses vanish. To determine strains at the point T at the line DF, we use the finite-element method [26]. The coordinates of the points D, T, and F at the line DF are related by the equation

$$\frac{y_T - y_F}{y_D - y_F} = \frac{x_T - x_F}{x_D - x_F} \qquad \text{or} \qquad y_T = \frac{y_D}{x_D}\, x_T. \tag{2}$$

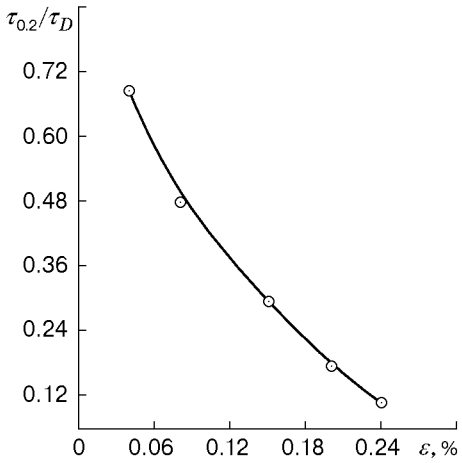

Fig. 3

Dividing Eq. (2) by l_0 (initial length of the specimen), we obtain the following relation between the relative displacements u_D and u_T at the points D and T:

$$u_T = (u_D/x_D)x_T, \qquad u_T = (x_T/x_D)u_D. \tag{3}$$

We consider the triangle DMF. Using the sine theorem, we obtain

$$|DF|/\cos\beta = |DM|/\cos(\alpha+\beta), \tag{4}$$

where $x_D = |DM|$ and β is the slope angle of the slip plane. Before deformation, we have $|DF| = |DE|$. Under compression along the line ND, the line DF is stretched. Provided the strain volume remains unchanged, the variation in the cross-sectional area is given by $S_\varepsilon = S_0\exp(+\varepsilon)$, whence $|DF| \approx |DE|\exp(+\varepsilon/2)$ (the plus denotes extension). For nonuniform strains at the line DF, this relation is approximate. Substituting the values of $|DF|$ and $|DM|$ into formulas (3) and (4), respectively, we obtain

$$\frac{x_T}{|DE|} = \frac{\cos(\alpha+\beta)}{\cos\beta}\exp\Big(+\frac{\varepsilon}{2}\Big)\frac{\varepsilon_T}{\varepsilon_D}. \tag{5}$$

We write Eq. (5) in terms of stresses. To this end, we assume that the relative displacements at the points N and T (Fig. 2b) occur in the region of elastic strains of the crystal lattice and, hence, they are proportional to stresses:

$$\frac{x_T}{|DE|} = \frac{\cos(\alpha+\beta)}{\cos\beta}\exp\Big(+\frac{\varepsilon}{2}\Big)\frac{\tau_T}{\tau_D}. \tag{6}$$

If the current stress at the point T is equal to the yield point, i.e., $\tau_T = \tau_{0.2}$, one can use formula (6) to estimate the yield-point distribution along the trace DF. The external stresses along the line DF decrease from maximum values at the point D equal to applied external stresses to minimum values at the point F.

In this case, $x_{0.2}/|DE|$ in (6) is the relative magnitude of the trace DF; at the segment DT of this trace, external stresses decrease to the yield point. The slope of the trace at the specimen edge was determined experimentally for different levels of strain. For the $[\bar{2}34]$ orientation, it was found that $\alpha = 1$, 2, 3, 5, and 8° and $\sigma_D = 68.8$, 99.0, 164.1, 273.7, and 427.0 MPa for the strain $\varepsilon = 4$, 8, 15, 20, and 24%, respectively. The yield point is $\tau_{0.2} = 46.9$ MPa. The calculation results are shown in Fig. 3. Along the line DF, the flow stresses decrease abruptly from $\sigma = 427$ MPa at the point D to the yield point at a distance of approximately $0.1|DF|$. This means that stresses acting on the remaining part of DF are too low to cause shear strain. Deformation in the shear zone can be caused only by long-range stresses of dislocations newly formed in a cluster, which shift previously formed dislocations toward the crystal surface. In this case, the stress fields are strongly nonuniform. The specific feature of this mechanism is that movable dislocations (see Fig. 2c) and the dislocation cluster 1–4 lie in the same slip plane, and shear along the trace TF is difficult to occur. It is likely that the revealed mechanism of slip termination is most pronounced at low temperatures ($T = 77$ K), since thermally activated processes are difficult to develop in this case. Dislocations are strongly attached to the shear zone, and, as a result, the long-range stresses must increase to shift the dislocations in the cluster to the specimen surface.

The relative displacements of the points N and T (see Fig. 2b) due to deformation can be expressed in terms of the conventional strain of the specimen $\varepsilon_{\text{conv}}$ at these points. Indeed, the strain at the point N is given by $(l_N - l_0)/l_0 = (l_0 - |ND| - l_0)/l_0 = -|ND|/l_0 = \varepsilon_{\text{conv}}$ and that at the point T is $(l_0 - y_T - l_0)/l_0 = -y_T/l_0 = \varepsilon_{\text{conv}}$ (the minus denotes compression). The relative displacements are equal to the conventional strains of the specimen at the points N and T.

The true strain ε and the conventional strain $\varepsilon_{\text{conv}}$ are related by the formula $\varepsilon = \ln(1 + \varepsilon_{\text{conv}})$ and differ only slightly for strains varied within 20%.

We use the finite-element method assuming that the line DF remains straight. The physical basis of this assumption is as follows. Rotation of the line DF corresponds to the plane problem. We calculate the ratio of the increments $u_T/\Delta x$ of the point T on the line DF (u_T is the displacement along the strain axis and Δx is the displacement in the perpendicular direction). For small angles α, this ratio is proportional to $\tan\alpha$ [27]. For a constant strain volume, we have

$$\frac{u_T}{\Delta x} \approx \frac{l_0 \exp(-\varepsilon) - l_0}{S_0^{0.5} \exp(+\varepsilon/2) - S_0^{0.5}}.$$

Passing to the limit as $\Delta x \to 0$, we obtain

$$l_0 \frac{d\varepsilon_{\text{conv}}}{dx} = l_0 \frac{\exp(-\varepsilon) - 1}{S_0^{0.5}(\exp(+\varepsilon/2) - 1)}, \qquad \frac{d\varepsilon_{\text{conv}}}{dx} = C \frac{\exp(-\varepsilon) - 1}{\exp(+\varepsilon/2) - 1}, \tag{7}$$

where $C = \text{const}$ and S_0 is the initial cross-sectional area of the specimen. Using the above-mentioned relation between the true and conventional strains, we write the solution of Eq. (7) in the form

$$2\exp(+3\varepsilon/2)3\exp(+\varepsilon) + 6\exp(+\varepsilon/2) - 6\ln(1 + \exp(+\varepsilon/2)) = -3Cx + D, \tag{8}$$

where $D = \text{const}$. Expanding the left side in (8) into a power series, we obtain

$$(5 - 6\ln 2) + 1.5\varepsilon + (57/16)\varepsilon^2 + \ldots = -3Cx + D.$$

For $\varepsilon = 19\%$, the quadratic term in the solution is smaller than the linear term by almost a factor of 3. Therefore, it can be assumed that the linear relation $\varepsilon = f(x)$ is valid, i.e., approximation of DF by a straight line in the finite-element method is physically justified. Retaining quadratic terms in (8), we obtain the parabolic relation $\varepsilon^2 = f(x)$.

Let us estimate the possible contribution of the reversed stress caused by dislocations accumulated at the specimen edge to deformation resistance and also the deviation from relation (1). A cluster of dislocations is formed along the slip trace DF (see Fig. 2b and c). In the tail of the cluster, the shear stresses approach the yield point. It is assumed that dislocations cannot slide at these stresses. The first dislocation ceases to move near the point T. The second dislocation that follows the first one (it also ceases to move near the point T) shifts the first dislocation along the trace at a distance where the sum of stresses of interaction between these dislocations and the external stress that acts on the first dislocation (this sum is smaller than the yield point, which is taken into account by the coefficient γ) becomes equal to the yield point. We write the condition of equilibrium for the first dislocation:

$$\gamma\tau_0 + Gb/(2\pi K x_1) \approx \tau_0. \tag{9}$$

Here x_1 is the distance between the first and second dislocations, τ_0 is the yield point, $\gamma\tau_0$ is the stress acting on the first dislocation, and $K = 1 - \nu$ (ν is Poisson's ratio). We estimate the distance x_1 at which the first dislocation is shifted toward DF. Obviously, the quantity γ is indeterminate. We assume that the first dislocation passed a distance such that the applied stresses decrease to 0.9 of the yield point ($\gamma = 0.9$). Consequently, Eq. (9) can be written in the form

$$Gb/(2\pi K x_1) \approx 0.1\tau_0. \tag{10}$$

We calculate the distance x_1 for the $[\bar{1}11]$ orientation. The shear modulus G is taken to be $8 \cdot 10^4$ MPa, $\nu = 1/3$, $b = 0.25$ nm, and the yield point is $\tau_0 \approx 55$ MPa. Substitution of these values into formula (10) yields $x_1 \approx 870$ nm. We consider the formation of the dislocation cluster in the slip trace DF and estimate the number of dislocations for the strain $\varepsilon \approx 19.5\%$. In this case, the shear stresses are $\tau \approx 165$ MPa. We write the equation of equilibrium of the nth dislocation near the point T (see Fig. 2c):

$$Gb/(2\pi K x_1)(1 + 1/2 + 1/3 + 1/4 + \ldots + 1/n) \approx \tau. \tag{11}$$

In formula (11), the following approximation is used. The dislocations in the cluster are distributed uniformly and the distance between them is equal to x_1. The bracketed numerical series is divergent. We find a partial sum of the series. For a sufficiently large number of terms, we have [17, 25]

$$S_n = 1 + \frac{1}{2} + \frac{1}{3} + \frac{1}{4} + \ldots + \frac{1}{n} \approx \int_1^n \frac{dn}{n} = \ln n. \tag{12}$$

More accurate estimates of the partial sum given in [25] show that $S_n \approx \ln n + 5.6$. Substituting the partial sum S_n from formula (12) into formula (11) and assuming that the applied stresses are equal to $\tau \approx 165$ MPa, we obtain the number of dislocations n in the cluster:

$$\mathrm{Ln}\, n \approx 2\pi(1-\nu)x_1\tau/(Gb) - 5.6.$$

For the parameters chosen, this formula yields $n \approx \exp(24.4) \approx 4 \cdot 10^{10}$. Obviously, this number of dislocations in the cluster DF is overestimated. Most of these dislocations arrive at the surface and form a rough trace. We estimate the possible number of dislocations, in the trace DF, that can be held by the first dislocation in the cluster. To this end, it is necessary to write the equation of equilibrium of the first dislocation (see Fig. 2c). This dislocation can retard the motion of $n-1$ subsequent dislocations in the cluster if superposition of paired interactions of all dislocations with applied stresses does not exceed the yield point for the first dislocation. Since the parameter γ is indeterminate, the calculations are approximate. Setting $\gamma = 0.1$, we obtain $\tau \approx \gamma\tau_0 = 0.1\tau_0$. The equation of equilibrium (11) becomes

$$0.1\tau_0 + Gb/(2\pi K x_1)(1 + 1/2 + 1/3 + 1/4 + \ldots + 1/n) \approx \tau_0.$$

Simple calculations yield $\mathrm{Ln}\, n \approx 9 - 5.6 = 3.4$. It follows that, for $\varepsilon = 19.5\%$ and $T = 77$ K, the number of dislocations in the cluster is $n \approx 30$. It is worth noting that the equidistant dislocation distribution in the cluster determines the lower boundary of the number of dislocations. Dislocations in the cluster DF are responsible for deviation from the linear relation $\tau = f(\rho^{0.5})$. Since the number of dislocations in the cluster depends on the dislocation density ρ, the contribution to deformation resistance at $T = 77$ K should be higher than that predicted by the linear relation $\tau = f(\rho^{0.5})$. We determine the contribution to deformation resistance using the Seeger formula [23]. This formula allows one to calculate the long-range stresses caused by clusters of dislocations at distances comparable with the average distance between dislocations:

$$\tau = Gb\sqrt{n}\rho^{1/2}/(2\pi K).$$

For $\varepsilon = 19.5\%$, we have $\rho \approx 10.4 \cdot 10^9$ cm^{-1}. The other parameters are listed above. The estimates show that $\tau \approx 266.9$ MPa. The contribution of clusters at the specimen edge to deformation resistance is rather considerable, compared to that of shear stresses. The stress calculated by the formula

$$\tau = Gb\rho^{1/2}\,\mathrm{Ln}\, n/(2\pi K),$$

which takes into account the stresses caused by clusters of dislocations, is equal to 165 MPa. An analysis of the number of dislocations in the cluster DF for other orientations shows that $n \approx 30$ for all the orientations. Even for the $[\bar{1}39]$ orientation, for which the yield point is approximately 1.5 times that for the $[\bar{1}11]$ orientation, this number is close to $n \approx 30$. An analysis of the image stresses τ_{im} that occur owing to the effect of the specimen surface and act on the head dislocation shows that they are negligible [17]: $\tau_{\mathrm{im}} = Gb/(4\pi(L_{\mathrm{surf}} - L_{\mathrm{cluster}})) \approx 1/6300$ MPa, where L_{surf} is the distance from the surface to the head dislocation and L_{cluster} is the length of the cluster ($L_{\mathrm{surf}} \approx 10^{-4}$ m and $L_{\mathrm{cluster}} \approx 2700$ nm for $T = 77$ K and $\varepsilon \approx 20\%$).

Thus, it has been shown that the contributions of dislocation clusters in the slip plane at the specimen edge to deformation resistance can have a considerable effect on flow stresses at low test temperatures ($T = 77$ K), which results in deviation from the linear relation $\tau = f(\rho^{0.5})$. The deviation from the linear relation is due to the fact that sliding dislocations are attached to their slip plane owing to weak thermally activated processes on dislocations.

REFERENCES

1. Yu. A. Abzaev, Yu. V. Solov'eva, É. V. Kozlov, et al., "Calculation of shear stresses in single crystals of the Ni_3Ge alloy," *Izv. Vyssh. Uchebn. Zaved., Fiz.*, No. 6, 48–53 (1995).
2. Yu. A. Abzaev, V. A. Starenchenko, Yu. V. Solov'eva, et al., "Analysis of fragmentation of deformation in Ni_3Ge single crystals," *J. Appl. Mech. Tech. Phys.*, **39**, No. 1, 135–139 (1998).
3. Yu. A. Abzaev, V. A. Starenchenko, N. A. Koneva, and É. V. Kozlov, "Evolution of the dislocation structure and hardening mechanisms of Ni_3Ge single crystals oriented for multiple slip," *Izv. Vyssh. Uchebn. Zaved., Fiz.*, No. 3, 65–70 (1987).
4. V. A. Starenchenko, Yu. A. Abzaev, and N. A. Koneva, "Stability loss of uniform plastic strain of Ni_3Ge single crystals," *Fiz. Met. Metalloved.*, **64**, No. 6, 1178–1182 (1987).
5. V. A. Starenchenko, Yu. A. Abzaev, N. A. Koneva, and É. V. Kozlov, "Thermal hardening and evolution of the dislocation structure of Ni_3Ge single crystals," *Fiz. Met. Metalloved.*, **68**, No. 3, 595–601 (1989).
6. V. A. Starenchenko and Yu. A. Abzaev, "Temperature dependence of parameters of interdislocation interaction in Ni_3Ge single crystals," *Metallofizika*, No. 2, 131–136 (1991).
7. V. A. Starenchenko, Yu. A. Abzaev, Yu. V. Solov'eva, and É. V. Kozlov, "Thermal hardening of Ni_3Ge single crystals," *Fiz. Met. Metalloved.*, **79**, No. 1, 147–155 (1995).
8. V. A. Starenchenko, Yu. V. Solov'eva, Yu. A. Abzaev, and B. I. Smirnov, "Orientation dependence of thermal hardening of single crystals of the Ni_3Ge alloy," *Fiz. Tverd. Tela*, No. 38, 3050–3058 (1996).
9. V. A. Starenchenko, Yu. V. Solov'eva, Yu. A. Abzaev, et al., "Evolution of the dislocation structure during deformation of Ni_3Ge single crystals of various orientations," *Fiz. Tverd. Tela*, **40**, No. 4, 81–89 (1998).
10. V. A. Starenchenko, Yu. V. Solov'eva, and Yu. A. Abzaev, "Accumulation of dislocations and thermal hardening in alloys with an $L1_2$ superstructure," *Fiz. Tverd. Tela*, **41**, No. 3, 454–460 (1999).
11. J. N. Lomer and H. M. Rozenberg, "The detection of dislocation by the temperature heat conductivity measurements," *Philos. Mag.*, **4**, No. 340, 467–483 (1959).
12. R. W. K. Honeycombe, *The Plastic Deformation of Metals*, Edward Arnold, London (1968).
13. J. Weertman and J. Wirtman, in: R. W. Cahn (ed.), *Physical Metallurgy*, North-Holland, Amsterdam (1956).
14. L. I. Mirkin, *Physical Fundamentals of Strength and Plasticity* [in Russian], Izd. Mosk. Univ., Moscow (1968).
15. D. McLean, *Mechanical Properties of Metals* John Wiley and Sons, New York–London (1962).
16. H. G. van Bueren, *Imperfections in Crystals*, North-Holland, Amsterdam (1960).
17. J. Fridel, *Dislocations*, Pergamon Press, Oxford (1964).
18. N. A. Koneva, L. A. Teplyakova, É. V. Kozlov, "Nature of hardening of ordered alloys with an $L1_2$ superstructure," in: *Structure and Plastic Behavior of Alloys* [in Russian], Izd. Tomsk. Univ., Tomsk (1983), pp. 74–99.
19. N. A. Koneva and É. V. Kozlov, "Nature of substructural hardening," *Izv. Vyssh. Uchebn. Zaved., Fiz.*, No. 8, 3–14 (1982).
20. N. A. Koneva and É. V. Kozlov, "Special features of substructural hardening," *Izv. Vyssh. Uchebn. Zaved., Fiz.*, No. 3, 56–70 (1991).
21. G. I. Taylor, "The mechanism of plastic deformation of crystals. Part 1. Theoretical," in: *Proc. Roy. Soc. London, Ser. A*, **145** (1934), pp. 362–387.
22. N. F. Mott, "The work hardening of metals," *Trans. AIME*, No. 6, 962–968 (1960).
23. A. Seeger, J. Diehl, S. Mader, and H. Rebstock, "Workhardening and worksoftening of face-centered cubic metal crystals," *Philos. Mag.*, **2**, No. 15, 323–350 (1957).
24. H.-R. Pak, T. Saburi, and S. Nenno, "The effect on the temperature dependence of yield stress in Ni_3Ge single crystals," *Trans. Jpn. Inst. Metals*, **19**, No. 1, 35–42 (1978).
25. A. A. Predvoditelev, "Possible ways to construct the hardening theory based on tests on dislocations," in: *Physics of Deformation Hardening of Single Crystals* [in Russian], Naukova Dumka, Kiev (1972), pp. 74–94.
26. L. J. Segerlind, *Applied Finite Element Analysis*, John Wiley and Sons, New York (1976).
27. L. D. Landau and E. M. Lifshitz, *Theory of Elasticity*, Pergamon Press, Oxford (1986).